

# Constraints on the flux of $\sim (10^{16} - 10^{17.5})$ eV cosmic photons from the EAS–MSU muon data

Yu. A. Fomin,<sup>1</sup> N. N. Kalmykov,<sup>1</sup> I. S. Karpikov,<sup>2</sup> G. V. Kulikov,<sup>1</sup>  
M. Yu. Kuznetsov,<sup>2</sup> G. I. Rubtsov,<sup>2</sup> V. P. Sulakov,<sup>1</sup> and S. V. Troitsky<sup>2,\*</sup>

<sup>1</sup>*D.V. Skobeltsyn Institute of Nuclear Physics,*

*M.V. Lomonosov Moscow State University, Moscow 119991, Russia*

<sup>2</sup>*Institute for Nuclear Research of the Russian Academy of Sciences,  
60th October Anniversary Prospect 7a, Moscow 117312, Russia*

## Abstract

Results of the search for  $\sim (10^{16} - 10^{17.5})$  eV primary cosmic-ray photons with the data of the Moscow State University (MSU) Extensive Air Shower (EAS) array are reported. The full-scale reanalysis of the data with modern simulations of the installation does not confirm previous indications of the excess of gamma-ray candidate events. Upper limits on the corresponding gamma-ray flux are presented. The limits are the most stringent published ones at energies  $\sim 10^{17}$  eV.

---

\* st@ms2.inr.ac.ru

## I. INTRODUCTION

Searches for astrophysical gamma rays with energies  $10^{15} \text{ eV} \lesssim E_\gamma \lesssim 10^{20} \text{ eV}$  attracted considerable attention for years [1, 2]. At these energies, photons interact with the atmosphere and produce extensive air showers (EAS) which may be detected by installations studying cosmic rays. The primary motivation for the studies includes multimessenger astronomy. Photons work as a diagnostic tool to distinguish between various models of the origin of energetic cosmic rays and neutrinos. In particular, because of the pair production on cosmic background radiation, the photon flux from extragalactic sources is strongly suppressed at sub-PeV to sub-EeV energies, and non-observation of gamma rays in this energy band would strongly favor the extragalactic origin of IceCube-detected astrophysical neutrinos over the Galactic models [3, 4]. At higher energies, non-observation of cosmogenic photons [5] would strongly constrain models with proton composition of cosmic rays with  $E \gtrsim 10^{19.5} \text{ eV}$ , see e.g. Refs. [6, 7]. Contrary, observation of high-energy photons may be a smoking-gun signal of new physics, including superheavy dark matter [8, 9] (see also Ref. [10] and, for a recent reanalysis, Ref. [11]), axion-like particles [12], or an ultimate test of Lorentz-invariance [13, 14].

For air-shower experiments, the main problem in the photon search is to separate gamma-ray induced events from the usual, hadron-induced air showers. One of the best discriminating variables is the muon number of a EAS, which is much lower in photon-induced events, compared to the bulk of showers. Indeed, a photon-induced shower develops by means of electromagnetic interactions mostly, and the only source of muons is provided by photonuclear reactions, which have a relatively small cross section. Contrary, in a hadron-induced shower, lots of muons are produced in decays of  $\pi$  mesons, born in hadronic interactions. Unfortunately, muon detectors are small or missing in many modern cosmic-ray experiments. Here, we take advantage of having a large muon detector in the EAS-MSU experiment and use its data to search for air showers poor in muons.

Previous preliminary studies indicated some excess of gamma-ray candidates in the EAS-MSU data with respect to the expected background [15–17]. These results invited for a detailed study of the data with state of art methods. This study has been performed: a full Monte-Carlo model of the data and the detector was constructed [18] which gives an excellent description of the surface-detector results [18] as well as of the bulk of muon-

detector data [19]. Here, we present the ultimate results of this study and consider muonless photon-candidate events. We will see that, within the present approach, no excess of these photon-like events is seen in the data. This allows us to put upper limits on the primary gamma-ray flux which are world-best at energies  $E_\gamma \sim 10^{17}$  eV.

The rest of the paper is organized as follows. In Sec. II, we briefly describe the installation, the data and the Monte-Carlo simulations used in this work; references to more detailed descriptions are given. We derive the main result of the paper, the limits on the gamma-ray flux, in Sec. III. In Sec. IV, we estimate systematic uncertainties of the result and compare it with other studies, including previous photon searches in the EAS-MSU experiment. We briefly conclude in Sec. V.

## II. DATA AND SIMULATIONS

The EAS-MSU experiment and the Monte-Carlo model are described in detail in the previous papers [18, 20]. The installation consists of 76 charged-particle detector stations, in which multiple Geiger-Mueller counters are located which determine the number of charged particles ( $N_e$ ) in a shower. The total number of Geiger-Mueller counters in the surface part of the installation is about 10,000. The total area of all Geiger-Mueller counters is  $\sim 250$  m<sup>2</sup>; the total area of the installation is  $\sim 0.5$  km<sup>2</sup>. In this work, we use the data of the large muon detector located at the center of the array at a depth of 40 meters of water equivalent underground corresponding to the threshold energy of 10 GeV for vertical muons. The muon detector had the total area of 36.4 m<sup>2</sup> and consisted of Geiger-Mueller counters with area of 0.033 m<sup>2</sup> each.

For the present study, we select events with the following cuts:

- the event passes the reconstruction procedure and the reconstruction quality criteria are satisfied [21];
- the age parameter of the EAS is in the range  $0.3 < S < 1.8$ ;
- the reconstructed zenith angle  $\theta$  is below  $30^\circ$ ;
- the distance between the reconstructed shower axis and the array center where the muon detector is located is  $R < 240$  m;

- the reconstructed shower size is  $N_e > 10^7$ ;
- out of 32 sections of the muon detector, at least 28 were operational.

The only difference with the cuts used in Ref. [19] is the lower  $N_e$  threshold which is chosen to cover a wider range of energies of potential photons. The extension of the  $N_e$  range requires a new comparison of data to Monte-Carlo to validate the simulations. The corresponding distributions of  $N_e$ , shower age  $S$ , core distance of the array center  $R$ , zenith angle  $\theta$  and muon density at 100 meters  $\rho_\mu(100)$  are shown in Appendix. With the account of the muon detector operation cut, we are left with 1204 days of data taking within 1984–1990. The data set contains 3148 events.

Following the previous studies, we consider the following criteria to select photon-candidate events: the muon detector is not triggered by the shower. However, low-energy protons do not always produce a sufficient number of muons in EAS to activate the muon detector, in particular, at large distances between the detector and the shower axis. To evaluate the background of muonless events from hadronic primaries, we make use of the full Monte-Carlo (MC) model of the EAS-MSU array described in Ref. [18]. It includes simulations of artificial air showers by the CORSIKA 7.4001 [22] package with the QGSJET-II-04 [23] high-energy hadronic interaction model, FLUKA 2011.2c [24] low-energy hadronic interaction model and EGS4 [25] electromagnetic model. Artificial EAS are recorded and processed identically to the experimental data. The Monte-Carlo simulations have been performed for proton and iron primaries, see Ref. [18] for details; a realistic composition was assumed to be a mixture of the two. The muon component of EAS is highly dependent on the primary composition, therefore the number of muonless background events depends on the assumed proton fraction. For this study, the primary composition has been determined in Ref. [19] by fitting the observed distribution of the muon densities. The assumed fraction of protons is  $46 \pm 6\%$ . We note that, as discussed in Ref. [19], it agrees well with the composition obtained from the EAS-MSU surface-detector data [18]. More details on the MC set with hadronic primaries may be found in Ref. [18].

We also need a MC simulation with gamma-ray primaries which is used to determine the efficiency of the installation for the gamma-ray detection, to relate the reconstructed  $N_e$  to the primary-photon energy  $E_\gamma$  and to account for the amount of photon showers which do not produce photon-candidate (that is, muonless) events. The simulation and reconstruction

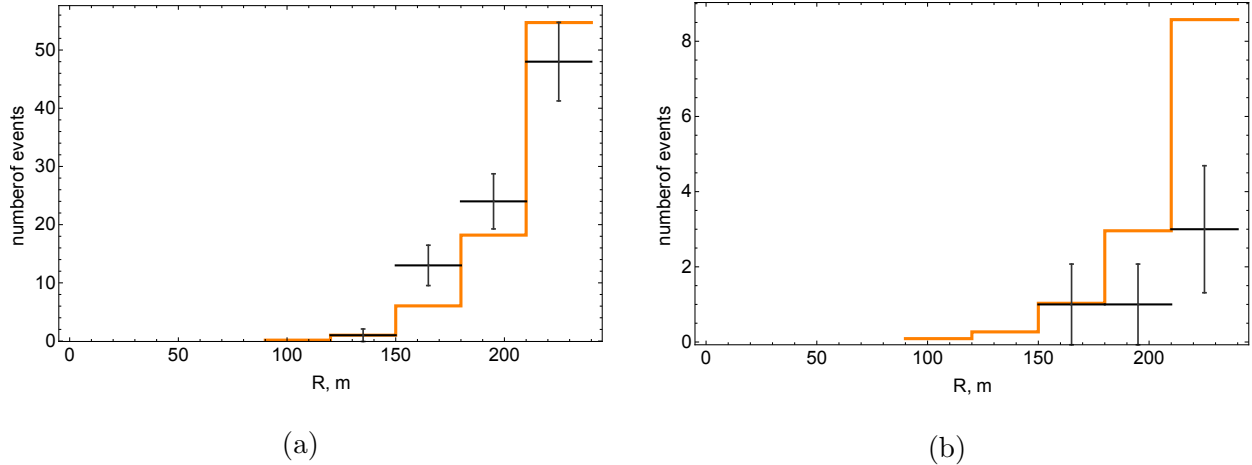


FIG. 1. Data versus MC comparison of the distribution of muonless events in  $R$ . Points with error bars: data, orange histogram: MC (mixed composition); (a):  $E_\gamma^{\min} > 2 \times 10^{16}$  eV; (b):  $E_\gamma^{\min} > 10^{17}$  eV.

of the artificial photon showers was performed in a way similar to that for hadron-induced events [18]. The total number of simulated independent gamma-induced showers is 300, their thrown energies follow the  $E_\gamma^{-1}$  spectrum with lower bound of MC  $10^{16} < E_\gamma \leq 10^{17.5}$  eV, and they are selected at the reconstruction stage to reproduce the primary spectrum  $\sim E_\gamma^{-2}$ , as is customary in high-energy photon searches. The dependence of the resulting limits on the assumed spectrum is through the efficiency only and is weak. The total number of MC realizations of gamma-induced events is 27310 (see Ref. [18] for description of the sampling). Of them, 3898 passed all cuts.

### III. THE GAMMA-RAY FLUX LIMIT

The total number of muonless events in the set is 86, while the expected number of background muonless events from primary hadrons is 80.1. The muon detector core distance distribution of the observed and expected muonless events is shown in Fig. 1.

To study various energy ranges, we consider certain subsamples of the data. The quantity reconstructed for each shower is  $N_e$ , not the primary energy  $E$ ; the relation between the two quantities may be obtained from simulations. The  $(E - N_e)$  relations are different for photons and for hadrons, and it is important to keep track of this difference for gamma-ray

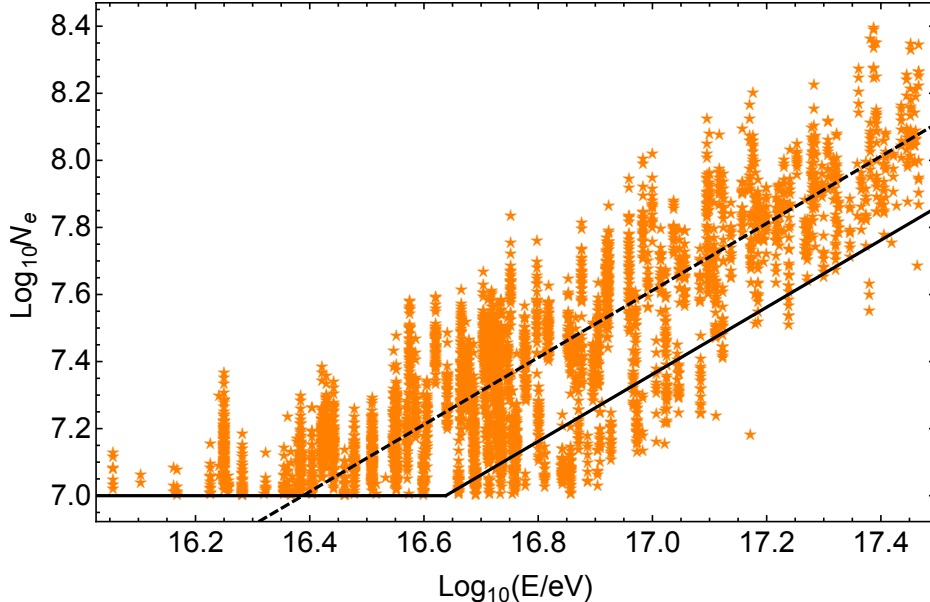


FIG. 2. The  $N_e(E_\gamma)$  relation. Stars – Monte-Carlo photons; dashed line – relation Eq. (1); full line bounds the region determined by the condition Eq. (2).

searches, see e.g. Refs. [10, 26]. The mean gamma-ray energy  $E_\gamma$  is related to  $N_e$  as

$$N_e(E_\gamma) = 4.1 \times 10^{-10} \frac{E_\gamma}{\text{eV}}, \quad (1)$$

see Fig. 2 for the MC simulated points and the fit. The condition used to select the data for the search of photons with  $E_\gamma > E_\gamma^{\min}$  is defined as

$$N_e > \max \{ 10^7, a N_e(E_\gamma^{\min}) \}, \quad (2)$$

where the coefficient  $a = 0.56$  was chosen in such a way that at least 90% of MC photon-induced showers with  $E_\gamma > E_\gamma^{\min}$  are reconstructed with these  $N_e$ .

For each energy cut  $E_\gamma^{\min}$ , we determine the number of observed muonless events,  $n_{\text{obs}}$ , in the sample, as well as the expected number of muonless events from the background of hadron-induced showers,  $n_b$ . No excess of muonless events is seen, and we estimate the maximum number of photon-induced events in the sample,  $n_\gamma^{\text{FC}}$ , by means of the standard Feldman–Cousins method for the Poisson distribution [27], for the 90% and 95% confidence levels (CL). The upper limits on the photon flux are then estimated as a ratio of  $n_\gamma^{\text{FC}}$  and the effective exposure of the experiment to photons of the given energy range. The effective exposure accounts for the fraction of photon events lost in the reconstruction and, also, of

reconstructed photon events which are not muonless. We estimate the effective exposure as follows.

The geometrical exposure for the conditions we use ( $R \leq R_{\max} = 240$  m,  $\theta \leq \theta_{\max} = 30^\circ$ ) is given by  $A_{\text{geom}} = \Omega \times S \times T$ , where  $\Omega = 2\pi(1 - \cos \theta_{\max})$  is the solid angle,  $S = \pi R_{\max}^2$  is the area and  $T = 14060.7$  hours is the on-time of the installation corresponding to the data set used. Note that the  $R$  cut is defined in the plane orthogonal to the shower axis and therefore  $\Omega$  is calculated differently from the conventional case when exposure is determined by the area of the array.

MC photon-induced showers are thrown in a square with area  $S_{\text{MC}} = (280 \text{ m})^2 = 0.3136 \text{ km}^2$  and with zenith angles up to  $\theta_{\text{MC}} = 35^\circ$ . The corresponding MC geometrical exposure is then  $A_{\text{MC}} = \Omega_{\text{MC}} \times S_{\text{MC}} \times T$ , where  $\Omega_{\text{MC}} = \pi \sin^2 \theta_{\text{MC}}$  and  $\theta_{\text{MC}} = 35^\circ$ . We calculate the number  $n_{\text{pass},0\mu}$  of events from the MC set which passed all cuts (that is, in particular, were reconstructed with geometrical properties corresponding to  $A_{\text{geom}}$ ), satisfy the criterion (2) and are muonless and divide it by the number  $n_{\text{MC}}$  of thrown MC events (corresponding to  $A_{\text{MC}}$ ). The effective exposure is then given by

$$A_{\text{eff}} = \frac{n_{\text{pass},0\mu}}{n_{\text{MC}}} A_{\text{MC}}. \quad (3)$$

The flux limit is then obtained as

$$I_\gamma = n_\gamma^{\text{FC}} / A_{\text{eff}},$$

where  $n_\gamma^{\text{FC}}$  corresponds to the required confidence level. Next, we define the exposure correction as a ratio of the effective exposure to geometrical one:

$$\xi = A_{\text{eff}} / A_{\text{geom}}. \quad (4)$$

Note that the exposure correction factor may exceed unity because Monte-Carlo events are thrown to the area larger than the installation. Figure 3 presents the exposure correction factor  $\xi$  as a function of energy. For comparison, the reconstruction efficiency for primary photons and protons is also shown (it is determined in a similar way as  $\xi$  but without the muonlessness condition and with the criterion  $N_e > 10^7$  instead of Eq. (2)). Decline of  $\xi$  at higher energies reflects the fact that the probability for a primary photon to produce a EAS which is not muonless grows with energy.

Our limits on the integral gamma-ray flux, which represent the main result of this work, are presented in Table I.

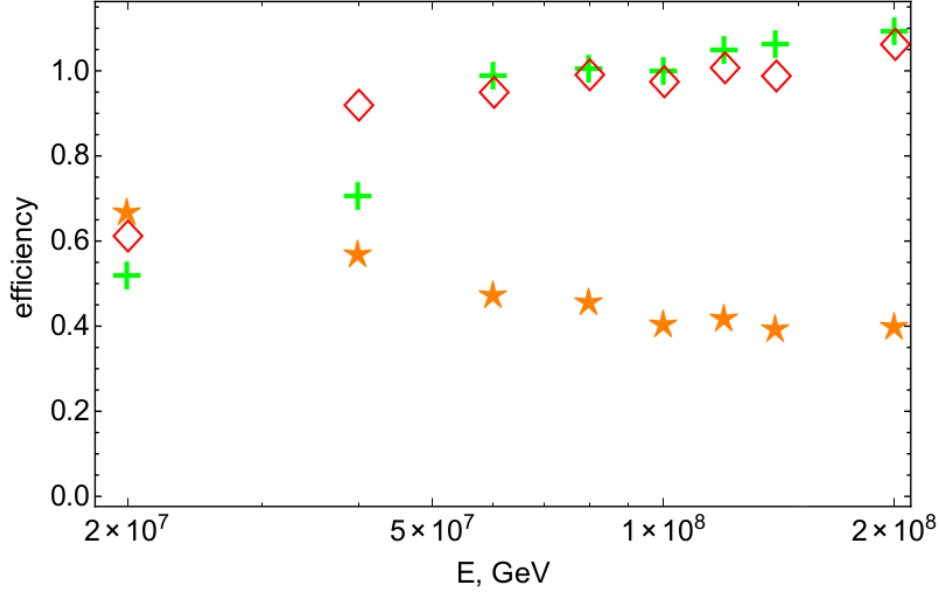


FIG. 3. The exposure correction factor  $\xi$  (stars) and the reconstruction efficiency for primary protons (pluses) and photons (diamonds) versus energy. See the text for more details.

$E_\gamma^{\min}$ , eV	$N_e^{\min}$	$n_{\text{obs}}$	$n_b$	$n_\gamma^{\text{FC}}$		$10^{16} \times A_{\text{eff}}, I_\gamma \times 10^{-16}, (\text{s}\cdot\text{cm}^2\cdot\text{sr})^{-1}$		
	$10^7$			(90% CL)	(95% CL)	( $\text{s}\cdot\text{m}^2\cdot\text{sr}$ )	(90% CL)	(95% CL)
$2 \times 10^{16}$	1	86	80.1	22.4	25.71	5.16	4.34	4.98
$4 \times 10^{16}$	1	86	80.1	22.4	25.71	4.39	5.09	5.85
$6 \times 10^{16}$	1.38	29	42.6	2.48	3.85	3.67	0.68	1.05
$8 \times 10^{16}$	1.84	9	21.7	1.26	2.13	3.53	0.36	0.6
$10^{17}$	2.3	5	12.9	1.21	1.84	3.14	0.39	0.58
$1.2 \times 10^{17}$	2.76	4	8.6	1.66	2.38	3.23	0.51	0.74
$1.4 \times 10^{17}$	3.22	2	5.6	1.44	2.16	3.05	0.47	0.71
$2 \times 10^{17}$	4.6	1	2.8	2	2.75	3.08	0.65	0.89

TABLE I. Upper limits on the integral diffuse gamma-ray flux  $I_\gamma$  at photon energies  $E_\gamma > E_\gamma^{\min}$ . The value of  $N_e^{\min}$  is determined by Eq. (2).  $n_{\text{obs}}$  is the number of observed muonless events with  $N_e > N_e^{\min}$ ;  $n_b$  is the expected number of background muonless events;  $n_\gamma^{\text{FC}}$  is the statistical upper limit on the excess of muonless events over the background;  $A_{\text{eff}}$  is the effective exposure for photons.  $n_\gamma^{\text{FC}}$  and  $I_\gamma$  are reported for two confidence levels, 90% and 95%, as indicated.



## IV. DISCUSSION

### A. Systematic uncertainties

The main part of systematic uncertainties in the study comes from the simulation of the background of muonless events from hadronic showers. Indeed, it is known that hadronic-interaction models used in the air-shower simulations are not perfect, in particular in the part related to the description of the muon content of EAS. While our previous study indicates [19] that the bulk of  $E > 10$  GeV muon data of the EAS-MSU experiment is well described by the QGSJET-II-04 simulations, assuming the primary chemical composition implied by the surface-detector studies, this is not directly tested for muon-poor showers. The uncertainties of the hadronic model, in principle, may reveal itself in the incorrect estimation of the background. Indeed, we note (cf. Table I) that for certain energy ranges, the number of observed muonless events in our sample is smaller than expected under the background-only hypothesis. Therefore, in addition to the standard statistical estimate of the upper limit on the gamma-ray flux, we calculated also the “expected” flux upper limits which would be obtained if the number of observed muonless events followed the simulations under the background-only hypothesis. Alternatively, one may estimate the flux limits which might be obtained under assumption that the MC model doesn’t provide a reliable prediction of the background. To this end, we use the “data-driven background”, that relies on the assumption that the correct background is equal to the number of the observed muonless events. These “expected” and “data-driven-background” limits on the gamma-ray flux are presented in Table II and compared in Fig.4.

We also estimate the systematic errors associated with the uncertainty of the chemical composition. The change of the proton fraction within its error  $\pm 6\%$  results in the energy dependent correction of flux limits. The variation of limits is 21% for the minimum energy and 4% for maximum energy.

A careful look at the relation between  $n_b$  and  $n_{obs}$  reveals one peculiarity which is most probably related to the modelling of hadronic interactions but, in principle, might also be explained in terms of the presence of a certain amount of primary photons. The ratio  $n_{obs}/n_b$  remains constant,  $\sim 0.4$ , for energies  $E_\gamma \gtrsim 8 \times 10^{16}$  eV, but quickly raises to  $\sim 1$  below this energy. If, due to some systematics in the modelling of the background, the real

$E_{\gamma}^{\text{min}}, \text{ eV}$	$I_{\gamma} \times 10^{16}, (\text{s}\cdot\text{cm}^2\cdot\text{sr})^{-1}$		
	expected main data-driven		
$2 \times 10^{16}$	3.08	4.34	3.20
$4 \times 10^{16}$	3.62	5.09	3.76
$6 \times 10^{15}$	3.12	0.68	2.73
$8 \times 10^{16}$	2.37	0.36	1.79
$10^{17}$	1.95	0.39	1.59
$1.2 \times 10^{17}$	1.67	0.51	1.42
$1.4 \times 10^{17}$	1.46	0.47	1.28
$2 \times 10^{17}$	1.04	0.65	1.09

TABLE II. Estimate of systematic uncertainties in the flux limits: the expected limits, the limits based on the data-driven background in comparison with the main result of the work (90% CL).

$n_b$  is indeed  $\sim 0.4$  of the MC one, then we have a certain excess of muonless events at  $2 \times 10^{16} \text{ eV} \lesssim E \lesssim 8 \times 10^{16} \text{ eV}$ , which may correspond to an excess of primary photons expected, for instance, in the heavy dark-matter decay scenario.

### B. Comparison with previous EAS-MSU results

Previous analyses of the EAS-MSU data in the same energy range suggested an excess of muonless events which might be explained by the presence of a certain amount of photons in the primary cosmic-ray flux at  $E \sim 10^{17} \text{ eV}$  [15–17]. The present study does not confirm that claim and puts strong upper limits on the gamma-ray flux, see Table I. It is therefore important to understand the differences between this analysis and the previous ones.

With respect to the previous preliminary analysis, this final study has several important advantages. First, it is based on the new full Monte-Carlo description of the air showers and of the installation [18]. This uses modern simulation tools and an analysis technique with the real and simulated events processed by one and the same reconstruction program. In such a way, we take into account all possible biases introduced at the reconstruction step, as well as keep track of rare fluctuations in the EAS development and registration. Second, the reconstruction program has been slightly revised for this study. The main

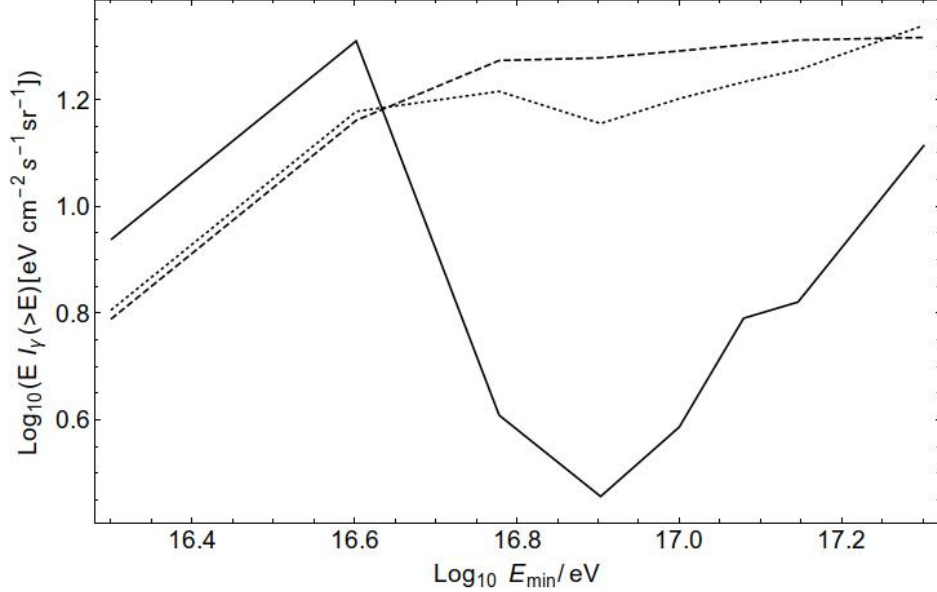


FIG. 4. Upper limits (90% CL) on the integral flux of gamma rays under various assumptions on the background: the MC background (full line); the data-driven background (dotted line); the expected exclusion (dashed line).

overall effect of the reconstruction update is that, while the muonless events remain in the data sample, their reconstructed energies become, for most of them, lower than before. For these lower energies, the background of muonless hadron-induced showers is higher, and the same amount of muonless events does no longer represent an excess. Third, an additional check of the quality of muon data was performed: at least 28 out of 32 sections of the muon detector are required to be operational.

To be specific, let us consider 48 muonless events with  $N_e \geq 2 \times 10^7$  studied in Ref. [16]. Of them, 28 events have  $N_e < 2 \times 10^7$  in the new analysis; 4 events arrived before 1984 (not included in the present data set); 10 events arrived at the days excluded from the present analysis because of stricter criteria on the quality of muon data; 6 muonless events remained in the data set. In addition, 3 new muonless events joined the data set in the new reconstruction (they did not pass the cuts in the old one), so the total number of muonless events with  $N_e \geq 2 \times 10^7$  is now 9. This reduced number of photon candidates is below the MC background expectation of 18.9 events, so no excess is present in the updated data set. Our new results are compared to previous studies in Fig.5.

Finally, the efficiency of the muonless detection of photons is estimated in the present

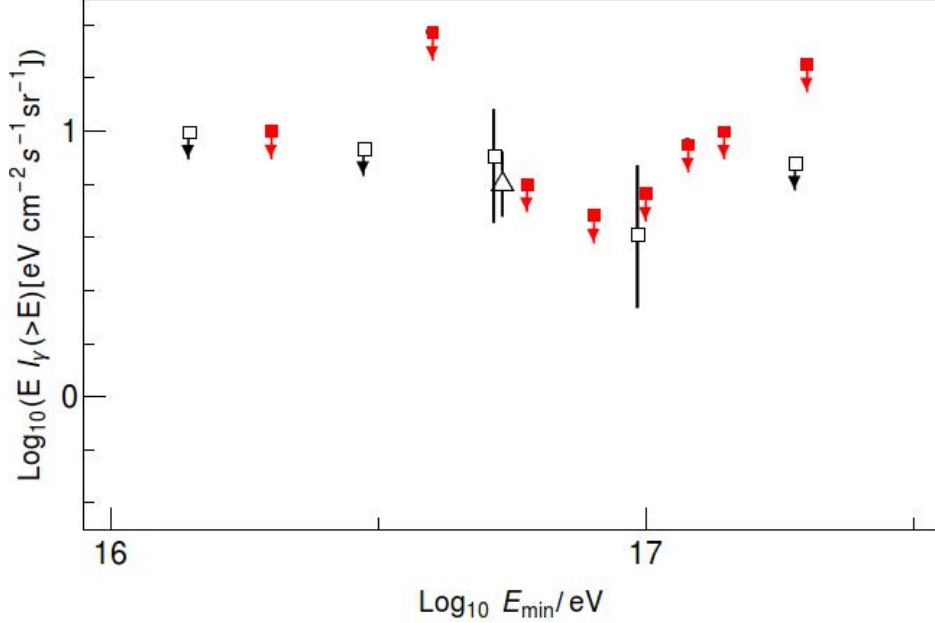


FIG. 5. Comparison of the present upper limits (95% CL) on the integral diffuse gamma-ray flux with previous EAS-MSU results. Full boxes (red online): this work; open boxes: Ref. [17]; open triangle: Ref. [16].

work with the full photon Monte-Carlo. The numerical values of limits became apparently weaker due to account of the fact that only about 40% of the photon-induced showers are registered as muonless.

### C. Comparison with other results and possible applications

Many experiments searched for primary photons with the EAS technique and none has yet found any. Our flux limits are compared to others in Fig. 6. We see that our limits are similar to those of the KASCADE-Grande experiment, being world-best for certain energies. At the same time, one can see that the energy range ( $10^{16} - 10^{18}$ ) eV discussed here is one of the least studied bands. While future studies to improve the limits are important, already the present data may be used to constrain astrophysical models with Galactic sources of PeV neutrinos [4] or decaying dark matter with appropriate mass and sufficiently hard spectrum (see [11] for a review).

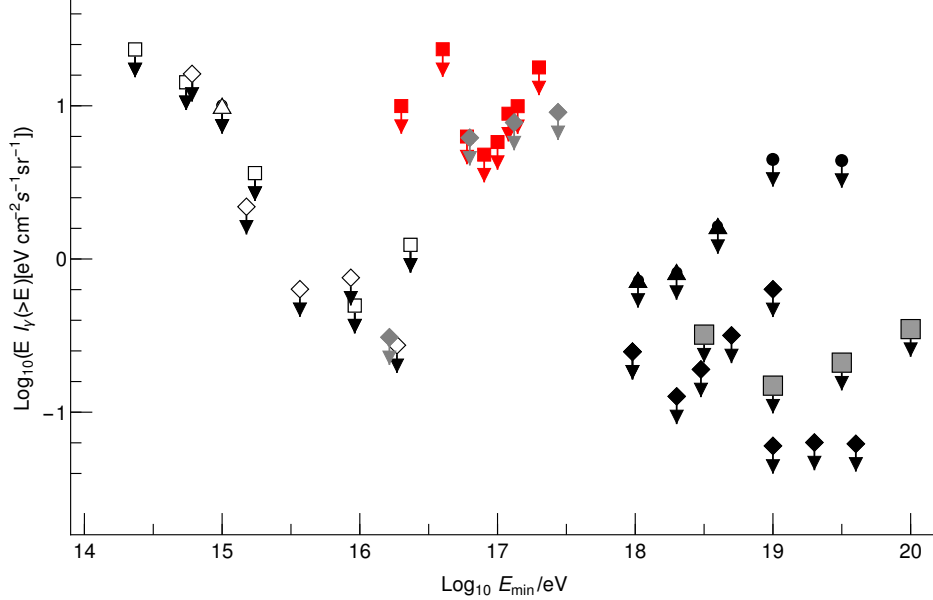


FIG. 6. Limits on the integral gamma-ray flux from PeV to ZeV. Full boxes (red online): this work; open triangles (EAS-TOP [28]), open boxes (CASA-MIA [29]), open diamonds (KASCADE [30]), gray diamonds (KASCADE-Grande [31], full triangles (Yakutsk [32]), full diamonds (Pierre Auger [33, 34]), full circles (AGASA [35]), large full boxes (Telescope Array [36]). All limits below  $10^{18}$  eV are 90% CL, all limits above  $10^{18}$  eV are 95% CL.

## V. CONCLUSIONS

This work presents the results of the search for primary photons in the EAS-MSU data. The photon candidate events are defined as ones giving no signal in the muon detector of the installation. We made use of the full Monte-Carlo simulation of the installation and of the updated reconstruction of EAS parameters. Contrary to the previous analysis of the same data, no evidence was found for an excess of photon-candidate events, and this fact allowed us to put upper limits on the diffuse flux of primary gamma rays at energies above  $\sim (10^{16} - 10^{17})$  eV. For certain energies, the limits are world-best ones. The difference with the previous study is, mainly, due to the change of reconstruction: the energies of muonless events moved downwards, while the background of muonless showers from primary hadrons is higher at lower energies. The limits obtained in this work may be used in multimessenger astrophysics as well as for constraining exotic particle-physics models.

## ACKNOWLEDGEMENTS

ST thanks J.-M. Frère for a discussion on the data-driven background and the Service de Physique Théorique at Université Libre de Bruxelles for hospitality at the final stages of the work. Monte-Carlo simulations have been performed at the computer cluster of the Theoretical Physics Department, Institute for Nuclear Research of the Russian Academy of Sciences. The experimental work of the EAS-MSU group is supported by the Government of the Russian Federation (agreement 14.B25.31.0010) and the Russian Foundation for Basic Research (project 14-02-00372). Development of the analysis methods and application of them to the EAS-MSU data is supported by the Russian Science Foundation (grant 14-12-01340).

- 
- [1] G.B. Khristiansen, G.V. Kulikov, Yu.A. Fomin, “Ultra-high-energy cosmic radiation”, Moscow, Atomizdat, 1975.
  - [2] M. Risse and P. Homola, “Search for ultrahigh energy photons using air showers,” *Mod. Phys. Lett. A* **22** (2007) 749 [astro-ph/0702632].
  - [3] M. Ahlers and K. Murase, “Probing the Galactic Origin of the IceCube Excess with Gamma-Rays,” *Phys. Rev. D* **90** (2014) 023010 [arXiv:1309.4077 [astro-ph.HE]].
  - [4] O. E. Kalashev and S. V. Troitsky, “IceCube astrophysical neutrinos without a spectral cutoff and  $10^{15}$ - $10^{17}$  eV cosmic gamma radiation,” *JETP Lett.* **100** (2015) 761 [*Pisma Zh. Eksp. Teor. Fiz.* **100** (2014) 865] [arXiv:1410.2600 [astro-ph.HE]].
  - [5] J. Wdowczyk, W. Traczyk, C. Adcock and A. W. Wolfendale, “The possibility of detectable fluxes of cosmic ray  $\gamma$  rays with energy above  $10^{19}$  eV”, *J. Phys. A: Gen. Phys.* **4** (1971) L37.
  - [6] G. Gelmini, O. E. Kalashev and D. V. Semikoz, “GZK photons as ultra high energy cosmic rays,” *J. Exp. Theor. Phys.* **106** (2008) 1061 [*Zh. Exp. Teor. Fiz.* **133** (2008) 1214] [astro-ph/0506128].
  - [7] D. Hooper, A. M. Taylor and S. Sarkar, “Cosmogenic photons as a test of ultra-high energy cosmic ray composition,” *Astropart. Phys.* **34** (2011) 340 [arXiv:1007.1306 [astro-ph.HE]].
  - [8] V. Berezhinsky, M. Kachelriess and A. Vilenkin, “Ultrahigh-energy cosmic rays without GZK cutoff,” *Phys. Rev. Lett.* **79** (1997) 4302 [astro-ph/9708217].

- [9] V. A. Kuzmin and V. A. Rubakov, “Ultra-high-energy cosmic rays: A Window to postinflationary reheating epoch of the universe?,” *Phys. Atom. Nucl.* **61** (1998) 1028 [astro-ph/9709187].
- [10] O. E. Kalashev, G. I. Rubtsov and S. V. Troitsky, “Sensitivity of cosmic-ray experiments to ultra-high-energy photons: reconstruction of the spectrum and limits on the superheavy dark matter,” *Phys. Rev. D* **80** (2009) 103006 [arXiv:0812.1020 [astro-ph]].
- [11] O. K. Kalashev and M. Y. Kuznetsov, “Constraining heavy decaying dark matter with the high energy gamma-ray limits,” *Phys. Rev. D* **94** (2016) 063535 [arXiv:1606.07354 [astro-ph.HE]].
- [12] M. Fairbairn, T. Rashba and S. V. Troitsky, “Photon-axion mixing and ultra-high-energy cosmic rays from BL Lac type objects – Shining light through the Universe,” *Phys. Rev. D* **84** (2011) 125019 [arXiv:0901.4085 [astro-ph.HE]].
- [13] M. Galaverni and G. Sigl, “Lorentz Violation in the Photon Sector and Ultra-High Energy Cosmic Rays,” *Phys. Rev. Lett.* **100** (2008) 021102 [arXiv:0708.1737 [astro-ph]].
- [14] G. Rubtsov, P. Satunin and S. Sibiryakov, “Prospective constraints on Lorentz violation from ultrahigh-energy photon detection,” *Phys. Rev. D* **89** (2014) 123011 [arXiv:1312.4368 [astro-ph.HE]].
- [15] N. Kalmykov, J. Cotzomi, V. Sulakov and Yu. Fomin, “Primary cosmic ray composition at energies from  $10^{17}$  to  $10^{18}$  eV according to the EAS MSU array data”, *Bull. Russ. Acad. Sci. Phys.* **73** (2009) 547 [*Izv. Ross. Akad. Nauk Ser. Fiz.* **73** (2009) 584]
- [16] Yu. A. Fomin et al., “Estimate of the fraction of primary photons in the cosmic-ray flux at energies  $\sim 10^{17}$  eV from the EAS-MSU experiment data,” *J. Exp. Theor. Phys.* **117** (2013) 1011 [*Zh. Exp. Teor. Fiz.* **144** (2013) 1153] [arXiv:1307.4988 [astro-ph.HE]].
- [17] Yu. A. Fomin et al., “Estimates of the cosmic gamma-ray flux at PeV to EeV energies from the EAS-MSU experiment data,” *JETP Lett.* **100** (2015) 699 [*Pisma Zh. Eksp. Teor. Fiz.* **100** (2014) 797] [arXiv:1410.2599 [astro-ph.HE]].
- [18] Yu. A. Fomin et al., “Full Monte-Carlo description of the Moscow State University Extensive Air Shower experiment,” *JINST* **11** (2016) T08005 [arXiv:1607.00309 [astro-ph.HE]].
- [19] Yu. A. Fomin et al., “No muon excess in extensive air showers at  $\sim 10^{17}$  eV primary energy: EAS-MSU muon versus surface detector data,” arXiv:1609.05764 [astro-ph.HE].
- [20] S. N. Vernov *et al.*, “New Installation Of Moscow State University For Studying Extensive Air Showers With Energies To  $10^{18}$  eV,” *Bull. Russ. Acad. Sci. Phys.* **44** (1980) 80 [*Izv. Ross. Akad. Nauk Ser. Fiz.* **44** (1980) 537].

- [21] G.B. Khristiansen, G.V. Kulikov, Yu.A. Fomin. *Cosmic Rays of Superhigh Energies*, Karl Tiemig Verlag, Munchen, 1980, 246 p.
- [22] D. Heck, G. Schatz, T. Thouw, J. Knapp and J. N. Capdevielle, “CORSIKA: A Monte Carlo code to simulate extensive air showers,” FZKA-6019.
- [23] S. Ostapchenko, “Monte Carlo treatment of hadronic interactions in enhanced Pomeron scheme: I. QGSJET-II model,” *Phys. Rev. D* **83** (2011) 014018 [arXiv:1010.1869 [hep-ph]].
- [24] G. Battistoni et al., “The FLUKA code: Description and benchmarking”, AIP Conf.Proc.896(2007) 31.
- [25] W. R. Nelson, H. Hirayama, D. W. O. Rogers, “The EGS4 code system”, Tech. Rep. 0265, SLAC (1985).
- [26] G. I. Rubtsov, L. G. Dedenko, G. F. Fedorova *et al.*, *Phys. Rev. D* **73** (2006) 063009 [astro-ph/0601449].
- [27] G. J. Feldman and R. D. Cousins, “A Unified approach to the classical statistical analysis of small signals,” *Phys. Rev. D* **57** (1998) 3873 [physics/9711021 [physics.data-an]].
- [28] M. Aglietta, B. Alessandro, P. Antoni *et al.* [EAS-TOP Collaboration], “A Limit to the rate of ultrahigh-energy gamma-rays in the primary cosmic radiation,” *Astropart. Phys.* **6** (1996) 71.
- [29] M. C. Chantell, C.E. Covault, J.W. Cronin *et al.* [CASA-MIA Collaboration], “Limits on the isotropic diffuse flux of ultrahigh-energy gamma radiation,” *Phys. Rev. Lett.* **79** (1997) 1805 [astro-ph/9705246].
- [30] Z. Feng *et al.* [KASCADE-Grande Collaboration], “Limits on the isotropic diffuse  $\gamma$ -rays at ultra high energies measured with KASCADE,” *PoS ICRC 2015* (2016) 823.
- [31] D. Kang *et al.* [KASCADE-Grande collaboration], “A limit on the diffuse gamma-rays measured with KASCADE-Grande,” *J. Phys. Conf. Ser.* **632** (2015) 012013.
- [32] A. V. Glushkov, I. T. Makarov, M. I. Pravdin *et al.*, “Constraints on the flux of primary cosmic-ray photons at energies  $E > 10^{18}$  eV from Yakutsk muon data,” *Phys. Rev. D* **82** (2010) 041101 [arXiv:0907.0374 [astro-ph.HE]].
- [33] A. Aab *et al.* [Pierre Auger Collaboration], “The Pierre Auger Observatory: Contributions to the 34th International Cosmic Ray Conference (ICRC 2015),” arXiv:1509.03732 [astro-ph.HE].
- [34] P. Abreu, M. Aglietta, E.J. Ahn *et al.* [Pierre Auger Collaboration], “The Pierre Auger Observatory III: Other Astrophysical Observations,” arXiv:1107.4805 [astro-ph.HE].



- [35] K. Shinozaki, M. Chikawa, M. Fukushima *et al.* [AGASA Collaboration], “Upper limit on gamma-ray flux above  $10^{19}$  eV estimated by the Akeno Giant Air Shower Array experiment,” *Astrophys. J.* **571** (2002) L117.
- [36] G. I. Rubtsov *et al.* [Telescope Array Collaboration], “Telescope Array search for photons and neutrinos with the surface detector data,” *PoS ICRC 2015* (2016) 331.

## APPENDIX. DISTRIBUTION OF EAS PARAMETERS FOR DATA AND MONTE-CARLO

In this appendix, we provide the data to Monte-Carlo comparison of the EAS parameter distribution for the extended cut  $N_e > 10^7$  used in the present work. The primary composition is the same as determined in Ref. [19] by fitting the observed distribution of the muon densities: 46% protons and 54% iron. The distributions of  $S$ ,  $N_e$ ,  $R$ ,  $\theta$  and muon density at 100 meters  $\rho_\mu(100)$  are shown in Figures 7-11. The validity of the  $N_e$  cut extension is verified by reasonable agreement of the data and Monte-Carlo.

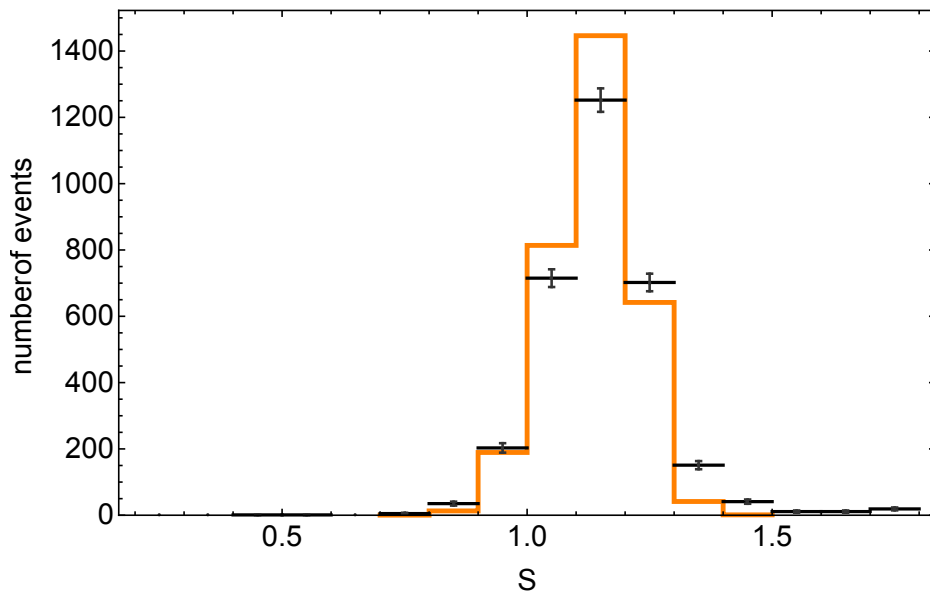


FIG. 7.  $S$  distribution for data (points) and MC (orange line).

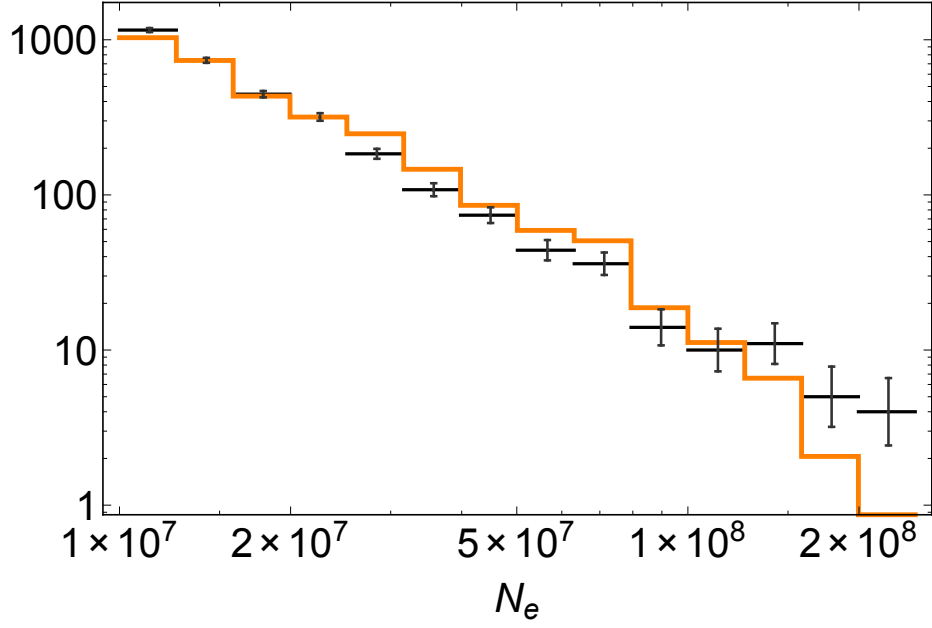


FIG. 8.  $N_e$  distribution for data (points) and MC (orange line).

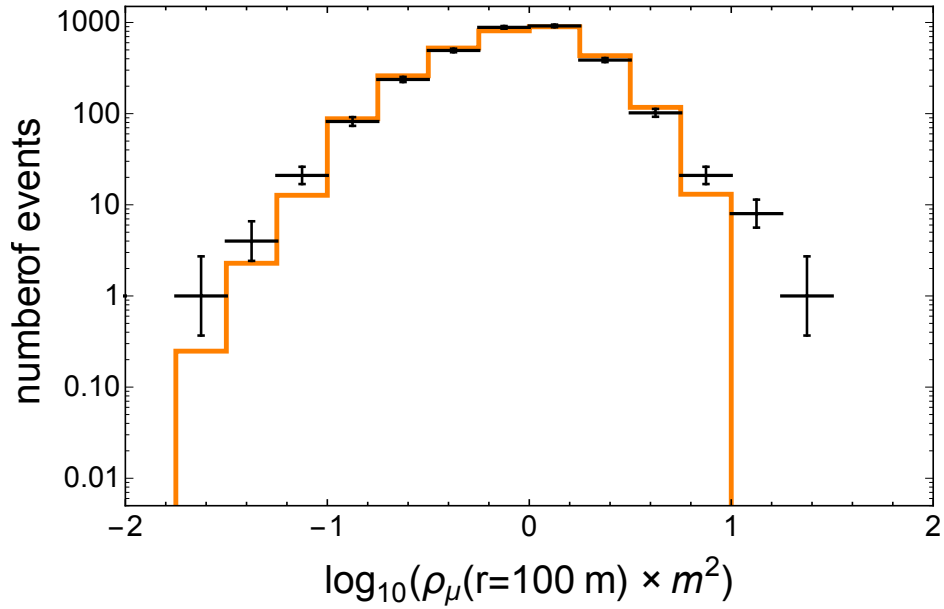


FIG. 9.  $\rho_\mu(100)$  distribution for data (points) and MC (orange line).

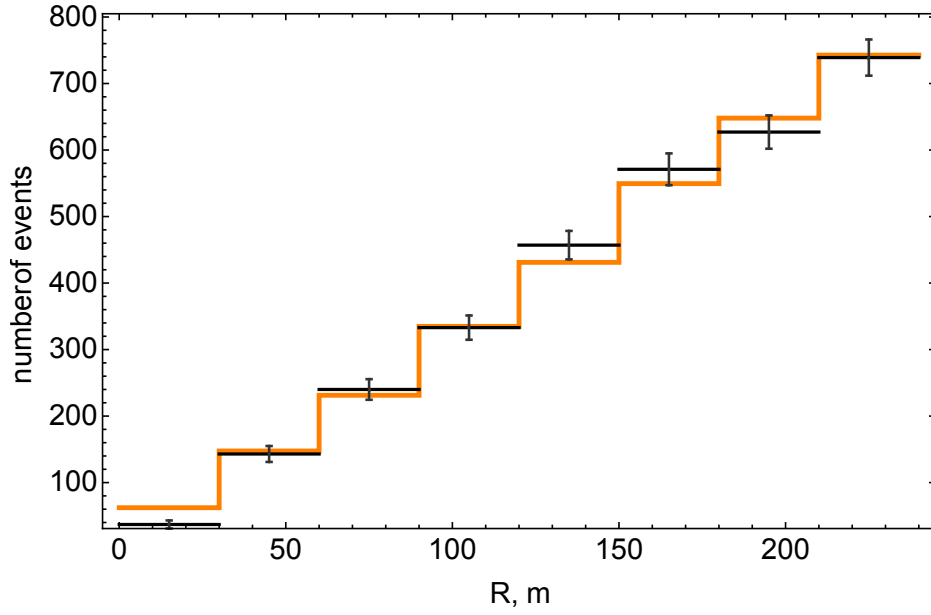


FIG. 10.  $R$  distribution for data (points) and MC (orange line).

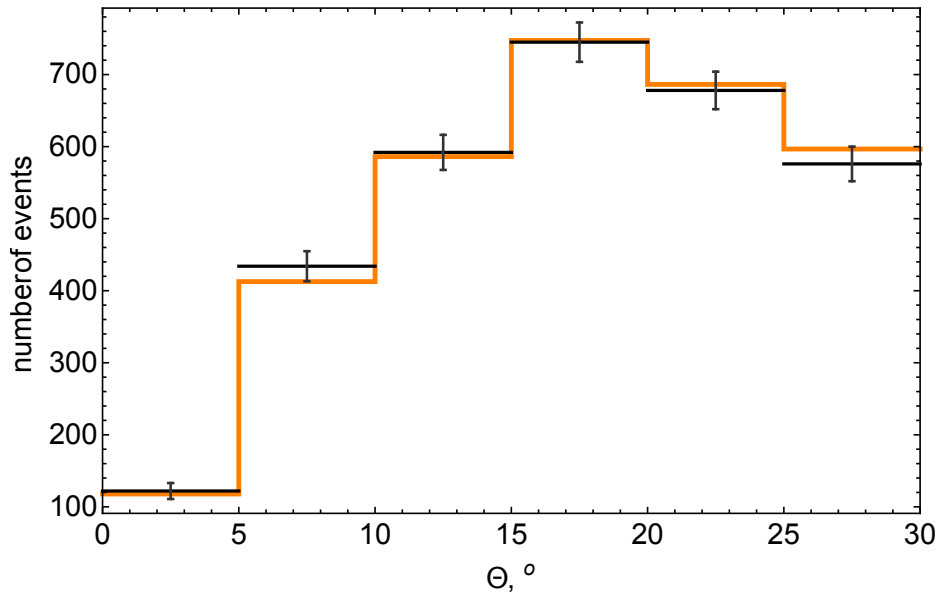


FIG. 11.  $\theta$  distribution for data (points) and MC (orange line).